Betacellulin (BTC) belongs to the epidermal growth factor (EGF)-like family of cytokines. Other mammalian EGF-like factors include EGF, transforming growth factor α (TGFα), heparin-binding EGF-like growth factor (HB-EGF), epiregulin (ER), amphiregulin (AR), epigen and a complex family of neuregulins (NRGs) [Dunbar and Goddard, 2000]. BTC and other EGF-like growth factors are synthesized as transmembrane proforms with an extracellular N-terminal ectodomain and a cytoplasmic C-terminus. The ectodomain is proteolytically cleaved to release a mature soluble factor in a process called ectodomain shedding [Sanderson et al., 2005]. The shed BTC ectodomain mediates diverse cellular responses such as proliferation, growth inhibition, migration, and differentiation [Dunbar and Goddard, 2000] via the binding of ErbB receptors, in particular ErbB1 (EGFR) and ErbB4 (HER4) [Olayioye et al., 2000].

Both genetic and biochemical experiments have implicated metalloprotease subtypes of the ADAM (a disintegrin and metalloprotease) [Blobel, 1997], membrane type matrix metalloprotease (MT-MMP) [Schlondorff et al., 2001], and matrix metalloprotease (MMP) [Li et al., 2002] families in the ectodomain shedding of a variety of transmembrane proteins. Previously, we and others have identified ADAM10 as the sole mediator of pro-BTC shedding in a range of different cell lines [Hinkle et al., 2004; Sahin et al., 2004; Sanderson et al., 2005]. This distinguishes BTC from other EGF-like factors including TGFα, HB-EGF, ER, AR, and several NRG isoforms which are predominantly ADAM17 substrates [Montero et al., 2000; Hinkle et al., 2004; Sahin et al., 2004; Horiuchi et al., 2005].

Shedding of pro-BTC and other EGF-like factors is up-regulated by chemical stimuli including the calcium ionophore A23187 and the metalloprotease activator APMA [Pandiella and Massague, 1991; Merlos-Suarez et al., 2001; Sanderson et al., 2005]. In addition, phorbol 12-myristate 13-acetate (PMA) exposure increases ectodomain shedding of most EGF-like factors with the exception of pro-BTC and possibly pro-EGF [Le Gall et al., 2003; Hinkle et al., 2004; Sahin et al., 2004; Sanderson et al., 2005]. PMA in particular remains one of the most widely scrutinized experimental activators of ectodomain shedding. However, for the most part, the physiological relevance of such stimuli to activated shedding events that may occur in vivo is poorly understood. On the other hand, endogenous or environmental stimuli such as G-protein coupled receptor (GPCR) agonists [Prenzel et al., 1999], cytokines [Tanida et al., 2004], cell adhesion [Gechtman et al., 1999], irradiation [Takenobu et al., 2003], reactive oxygen species (ROS) [Zhang et al., 2001], carcinogens [Richter et al., 2002], wounding [Xu et al., 2004], or infectious agents [Lemjabbar and Basbaum, 2002] can also stimulate shedding of transmembrane molecules and these enhanced shedding events are of physiological relevance.

It has become apparent that ectodomain shedding stimuli lead to transactivation of ErbB receptors. This is a process whereby stimuli increase the activity of sheddases, such as ADAMs [Prenzel et al., 1999] or MMPs [Hao et al., 2004], leading to EGF-like factor shedding and subsequent binding of the shed ectodomain to ErbB receptors, in either an autocrine or paracrine fashion. In most cases this leads to cellular effects such as proliferation, migration, or inhibition of apoptosis [Fischer et al., 2003; Zhang et al., 2004]. Transactivation has been most widely described with HB-EGF and TGFα [Wetzker and Bohmer, 2003] but in at least one report the glucagon-like peptide 1 (GLP-1) was proposed to stimulate pro-BTC shedding and ErbB1 transactivation at the surface of insulinoma cells [Buteau et al., 2003]. In some cases, transactivation of ErbB receptors in response to stimuli has been linked to pathophysiological processes such as atherosclerosis, chronic kidney disease, and cancer [Higashiyama, 2004; Lautrette et al., 2005].

In this report, the action of physiologically relevant stimuli such as GPCR agonists and ROS on the rate of metalloprotease mediated pro-BTC ectodomain shedding was investigated. We identify endothelin-1 (ET-1) and hydrogen peroxide (H_2O_2) as novel pro-BTC shedding stimuli. In addition, we show that H_2O_2 and calcium ionophore (A23187) are unique in their mechanisms of metalloprotease activation by relying on ROS and calcium influx, respectively. We also identify ADAM10 and ADAM17 as ET-1-activated pro-BTC sheddases, providing the first cellular evidence that ADAM17 may be involved in pro-BTC processing. These findings indicate that stimuli which relate to normal and pathophysiological processes dependent on ET-1 and ROS may function in

part via enhanced shedding of ErbB ligands such as BTC.

EXPERIMENTAL PROCEDURES

Materials

Anti-human BTC ectodomain Asp^{32}–Tyr^{111} polyclonal (antigen purified) antibody, mouse anti-human BTC ectodomain antibody, and recombinant human BTC were purchased from R&D Systems (Minneapolis, MN). A23187, phorbol 12-myristate 13-acetate (PMA), *p*-aminophenylmercuric acetate (APMA), and N-acetyl-L-cysteine were purchased from Sigma-Aldrich. TAPI-0 was purchased from Peptides International (Louisville, KY). GM6001, the MMP2/MMP9 inhibitor (2R)-2-[(4-biphenylylsulfonyl) amino]-3-phenylpropionic acid, the MMP3 inhibitor N-isobutyl-N-(4-methoxyphenylsulfonyl) glycylhydroxamic acid and all other inhibitors were purchased from Calbiochem (Merck, Darmstadt, Germany). ET-1 was obtained form Bachem (Torrance, CA).

Generation of an Antibody Against the Human Pro-BTC C-Terminus

New Zealand white rabbits were injected with the peptide DITPINEDIEETNIA corresponding to the human pro-BTC C-terminal residues Asp^{164}–Ala^{178}. The peptide was generated by Mimotopes Pty Ltd (Victoria, Australia) and was conjugated to the Diphtheria Toxoid super antigen [Del Giudice et al., 1998]. Conjugation required the additional presence of a cysteine residue at the N-terminus of the peptide. The first immunization was performed by subcutaneous injection of 300 μg of peptide conjugate mixed with 600 μl of Freund's complete adjuvant (Sigma-Aldrich). Subsequent immunizations were performed at 2-week intervals with 300 μg of peptide conjugant in sterile water. Following four immunizations, rabbits were bled for serum collection. Antibody generation was approved by the Animal Ethics Committee of the Women's and Children's Hospital, Adelaide, SA, Australia.

Cell Culture and Harvesting of Conditioned Media and Cell Lysates

The MB52 cell line is derived from the stable transfection of MCF7 human breast epithelial adenocarcinoma cells with the human pro-BTC cDNA [Tada et al., 1999]. Generation and propagation of wild-type and $ADAM17^{\Delta Zn/\Delta Zn}$ conditionally immortalized stomach epithelial (STOM) cells transduced with a retroviral vector for expression of C-terminally HA tagged pro-BTC have been described previously [Sanderson et al., 2005]. Rodent vascular smooth muscle cells (VSMCs) were obtained from Dr. Satoru Eguchi (Temple University School of Medicine, PA) and were transduced with the same pro-BTC retroviral vector as described [Sanderson et al., 2005]. MB52 and VSMCs were cultured at 37°C in Dulbecco's modified Eagle's medium (DMEM) supplemented with 10% fetal bovine serum (FBS), and penicillin/streptomycin/fungizone (PSF).

CM was harvested and then centrifuged at 12,000*g* to remove particulates. Soluble/shed BTC in CM was detected using the BTC EIA or ELISA and/or Western blot (see below). Cells were lysed directly in 2 × Tris-tricine PAGE loading buffer (0.9 M Tris-HCl, 24% Glycerol, 8% SDS, 0.015% Coomassie blue G, 5% β-mercaptoethanol, pH 8.45). Lysates were then heated at 95°C for 5 min, sheared five times through a 25 × 1″ gauge needle, and then centrifuged at 12,000*g* for 10 min to remove insoluble material. Cell lysates were used in Western blots.

BTC Enzyme-Linked Immunoassay (EIA) and ELISA

In experiments in which two or more alternate cell lines were used, soluble/shed BTC in CM was detected using the BTC ELISA as described previously [Sanderson et al., 2005]. Using this assay, levels of pro-BTC expression could also be determined in cell lysates and results showing levels of soluble/shed BTC in CM could be standardized based on this determination. In experiments involving a single cell line, the BTC EIA was sufficient to measure levels of soluble/shed BTC in CM. This assay was performed as described below. Ninety microliters of CM was mixed with 10 μl of 10 × EIA coating buffer (0.15 M Na_2CO_3, 0.35 M $NaHCO_3$, pH 9.3) and loaded into 96-well immunosorbent plates. Plates were coated overnight at 47°C and then blocked in 2% BSA in phosphate buffered saline-tween (PBS-T) (136 mM NaCl, 2.6 mM KCl, 1.5 mM KH_2PO_4, 8 mM Na_2HPO_4, pH 7.4, 0.1% Tween-20). The primary antibody (anti-human BTC ectodomain Asp^{32}–Tyr^{111}) was used at 0.2 μg/ml dilution and secondary HRP conjugated rabbit anti-goat antibody used at 1/1,000, diluted in PBS-T.

Plates were washed four times with PBS-T between antibody additions. EIAs were developed with OPD substrate (1 mg/ml o-phenylamine diamine) in citrate-phosphate buffer (35 mM citric acid, 67 mM Na_2HPO_4, pH 5.0, plus 0.03% H_2O_2) and stopped with 2 N H_2SO_4. Absorbance was read at 490 nm. Results are expressed as the mean percentage levels of BTC in CM compared to controls +/− standard deviation (SD) of triplicate determinations.

Concentration of BTC From Conditioned Media

The levels of soluble/shed BTC in CM were not sufficient to be detected by Western blot; therefore, BTC was precipitated using heparin-agarose beads as a means of concentration. Cells were grown to confluence in DMEM/10% FBS/PSF, then transferred to serum-free DMEM and cultured for 24 and 48 h before CM collection. BTC was precipitated from CM by addition of 20 µl of heparin-agarose (50% slurry). This was incubated overnight at 4°C and then pellets were collected by centrifugation at 10,000*g* for 10 min at 4°C. Pellets were washed three times with 1 ml of 20 mM Tris pH 7.5, and then centrifuged as above. BTC was eluted from the pellets by heating at 95°C for 5 min in 2 × Tris-tricine PAGE loading buffer prior to Western blotting.

Western Blotting

Cell lysates and CM were run on 10–20% gradient Tris-tricine polyacrylamide gels (Invitrogen). Proteins were then transferred to Hybond-C extra nitrocellulose (Amersham Pharmacia Biotech). Membranes were then blocked in 5% non-fat milk in Tris-buffered saline-tween (TBS-T) (25 mM Tris-HCl, 500 mM NaCl, pH 7.5, 0.1% Tween-20). Anti-human BTC ectodomain Asp^{32}–Tyr^{111} was used at 0.2 µg/ml dilution and anti-BTC C-terminus Asp^{164}–Ala^{178} serum was used at a 1/500 dilution. Secondary-horse radish peroxidase (HRP) conjugated antibodies were used at a 1/2,500 dilution. Following primary and secondary antibody additions, membranes were washed four times for 5 min with TBS-T. Blots were developed using Supersignal West Dura Extended Duration Substrate (Pierce, Milwaukee, WI). In some cases, nitrocellulose membranes were stripped by immersing in stripping buffer (60 mM Tris-HCl, 2% SDS, 1% β-mercaptoethanol, pH 6.8) at 65°C for 30 min, then blocked and re-probed with another antibody.

Inhibition of Constitutive Pro-BTC Shedding

For determination of the effect of protease inhibitors on constitutive shedding, cells were seeded into 6-well (VSMCs) or 24-well (MB52 cells) plates and grown to confluence. Cells were then cultured for 24 or 48 h in serum-free DMEM plus either the vehicle (DMSO) or protease inhibitor. Cell lysates and CM were harvested and analyzed by Western blot and the BTC EIA or ELISA.

Activation of Pro-BTC Shedding

For investigation of the effect of activators on pro-BTC shedding, cells were grown to confluence in 24-well (MB52 cells) or 6-well (STOM cells) plates. Cells were serum-starved for 2 h then cultured for 4 h in DMEM with either vehicle (DMSO) or an activator of shedding. Pre-incubations of cells with protease inhibitors, N-acetyl-L-cysteine or calcium-free DMEM were performed for 30 min prior to addition of shedding activators. For investigation of the effect of GPCR agonists on pro-BTC shedding in VSMCs, cells were grown to confluence in 6-well plates. Cells were then incubated twice in 3 ml serum-free DMEM for 24 h (total 48 h). This was performed in order to make cells quiescent by serum deprivation. Cells were then cultured in 900 µl DMEM for 30 min and then activated by direct addition of 100 µl of a 10 × solution of shedding activators to the culture medium. Cells were then incubated for 1 h prior to collection of CM and cell lysates for analysis using the BTC ELISA.

RESULTS

Characterization of Pro-BTC Ectodomain Shedding in MB52 Cells

We have previously identified the calcium ionophore A23187 and the metalloprotease activator APMA as stimuli that activate the ADAM10-dependent shedding of pro-BTC in conditionally immortalized cell lines [Sanderson et al., 2005]. We investigated here the possibility that ectodomain shedding of pro-BTC would occur in response to physiologically relevant stimuli. We used MB52 cells which are transfected to overexpress human pro-BTC [Tada et al., 1999] and initially performed experiments to determine if the ectodomain shedding of pro-BTC was functional in these cells.

We used a commercial anti-BTC ectodomain Asp^{32}–Tyr^{111} antibody and an anti-BTC C-terminus Asp^{164}–Ala^{178} antibody, which we generated, in order to characterize the BTC protein bands in MB52 cells lysates. The specificity of the anti-BTC C-terminus Asp^{164}–Ala^{178} antibody was confirmed by its ability to detect, by Western blot, pro-BTC in MB52 cells (transfected with pro-BTC) but not in the parental MCF7 cells (data not shown). Consistent with previous reports, five characteristic BTC bands of 40, 30, 25, 19, and 12 kDa were identified by Western blot analysis of MB52 cell lysates using the anti-BTC C-terminus Asp^{164}–Ala^{178} antibody (Fig. 1A) [Shing et al., 1993; Watanabe et al., 1994; Sanderson et al., 2005]. However, only the four largest bands were detected using the anti-BTC ectodomain Asp^{32}–Tyr^{111} antibody, indicating that the smallest 12 kDa band was the BTC cytoplasmic remnant which is generated following ectodomain shedding.

BTC shedding was confirmed by analysis of shed/soluble BTC isoforms in CM. Three BTC ectodomains (28, 15, 7 kDa) were identified using the anti-BTC ectodomain Asp^{32}–Tyr^{111} antibody (Fig. 1B). The inability to detect these soluble forms with an anti-BTC C-terminus Asp^{164}–Ala^{178} antibody indicated that these BTC species are most likely generated by ectodomain shedding (data not shown). Similar soluble BTC forms have been identified previously in the CM of mouse A9 fibroblast cells transfected with pro-BTC [Watanabe et al., 1994]. The 7 kDa shed BTC isoform was by far the most abundantly represented species. This is in stark contrast to results in conditionally immortalized cells in which the 28 kDa shed BTC species is virtually represented alone in CM [Sanderson et al., 2005].

To determine the involvement of different protease subtypes in pro-BTC shedding in MB52 cells, cells were cultured for 48 h in serum free DMEM with or without protease inhibitors and the level of shed BTC in CM evaluated using the BTC EIA. Only the broad-spectrum metalloprotease inhibitors GM6001 and TAPI-0 reduced the level of BTC ectodomains detected in CM (Fig. 1C, left panel). This was found to occur in a dose-dependent fashion with a peak inhibition between 50–100 μM for each compound (data not shown). Accordingly, Western blot analysis indicated that incubation with GM6001 or TAPI-0 resulted in a decrease in the level of the 12 kDa BTC cytoplasmic remnant as well as the 25 and 19 kDa pro-BTC forms, which are generated by N-terminal processing of the 40 kDa pro-BTC form (Fig. 1C, right panel) [Sanderson et al., 2005]. Concurrently, there was an accumulation of the major cell surface 40 kDa pro-BTC form. Together these results indicate that in MB52 cells, pro-BTC undergoes efficient metalloprotease-dependent ectodomain shedding and that these cells are a suitable experimental system for investigation of this process.

Metalloprotease-Dependent Pro-BTC Shedding is Activated by Hydrogen Peroxide

Whilst the ability of pharmacological agents including A23187 and APMA to induce pro-BTC ectodomain shedding in vitro has been clearly established [Sanderson et al., 2005], the role of physiological stimuli is unclear. Hydrogen peroxide (H_2O_2) is a generator of oxidative stress and is involved in a variety of physiological processes such as signal transduction through GPCRs and growth factor receptors as well as pathophysiological processes such as cancer, angiogenesis, and hypertension [Slupphaug et al., 2003; Touyz, 2003; Touyz et al., 2004; Ushio-Fukai and Alexander, 2004]. Short-term (4 h) treatment of MB52 cells with 1 mM H_2O_2 led to an increase in levels of soluble/shed BTC ectodomains in CM (Fig. 2A), as measured using the BTC EIA. This effect was approximately twofold higher than that observed for the previously established pro-BTC shedding stimuli APMA and A23187. Treatment with all stimuli led to a decrease in levels of the 40 kDa pro-BTC isoform and an increase in the level of the 12 kDa cytoplasmic remnant, indicating that pro-BTC shedding was activated (Fig. 2B). Levels of the 25 kDa pro-BTC band were also increased by pro-BTC shedding activators. This indicates that unlike in conditionally immortalized cells, these stimuli activate N-terminal proteolysis of the 40 kDa major pro-BTC form to a similar extent to the activation of ectodomain shedding in MB52 cells.

Pre-incubation of MB52 cells with the broad-spectrum metalloprotease inhibitor TAPI-0, but not specific inhibitors of MMP2 and MMP9 or MMP3, blocked the shedding of BTC ectodomains into CM as measured using the BTC EIA (Fig. 3A). Consistent with an inhibition of ectodomain shedding, Western analysis of lysates using the anti-BTC C-terminus

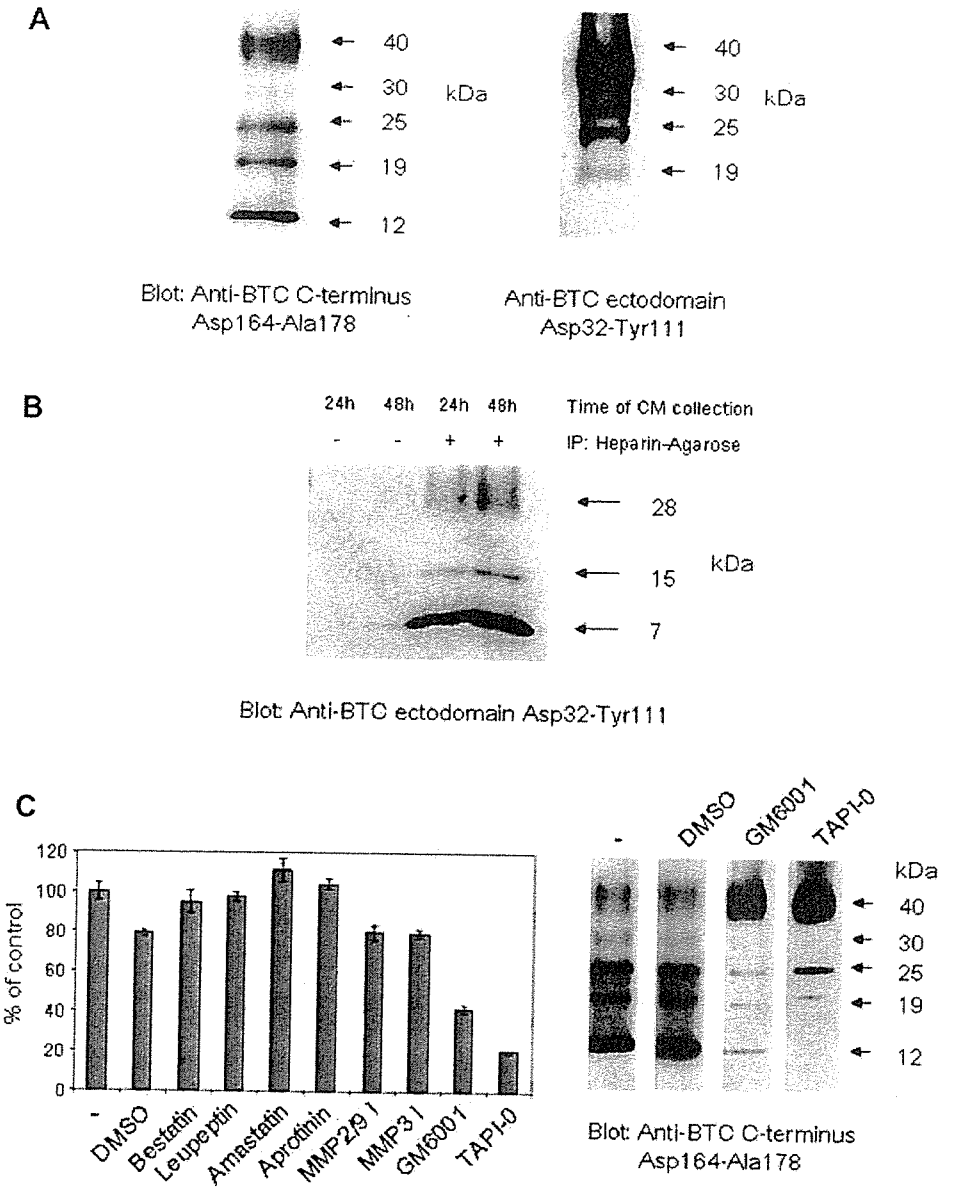

Fig. 1. Characterization of pro-BTC ectodomain shedding in MB52 cells. **A:** MB52 cell lysates were analyzed by Western blot using the anti-BTC C-terminus Asp^{164}–Ala^{178} antibody (left) and anti-BTC ectodomain Asp^{32}–Tyr^{111} antibody (right). The anti-BTC ectodomain Asp^{32}–Tyr^{111} antibody blot was overexposed in order to detect the 19 kDa cellular pro-BTC form. This band was weakly detected by the anti-BTC ectodomain Asp^{32}–Tyr^{111} antibody indicating that it most likely contains less of the ectodomain sequence than the larger 40 kDa pro-BTC species, owing to N-terminal proteolysis. **B:** MB52 cells were cultured in DMEM for 24 and 48 h and CM collected. Soluble/shed BTC ectodomains were concentrated using heparin-agarose beads. The molecular sizes of neat or concentrated BTC ectodomains in CM was analyzed by Western blot with the anti-BTC ectodomain Asp^{32}–Tyr^{111} antibody. **C:** MB52 cells were cultured for 48 h in the presence or absence of DMSO (vehicle) or inhibitors of aminopeptidases (bestatin or amastatin at 10 μM) [Ino et al., 2000; Scornik and Botbol, 2001], serine and cysteine proteases (leupeptin at 100 μM) [McConnell et al., 1993], trypsin, chymotrypsin, kallikrein, and plasmin (aprotinin at 2 μg/ml) [Trautschold et al., 1966], MMP2 and MMP9 ((2R)-2-[(4-biphenylylsulfonyl) amino]-3-phenylpropionic acid at 10 μM) [Tamura et al., 1998], MMP3 (N-isobutyl-N-(4-methoxyphenyl-sulfonyl) glycylhydroxamic acid at 10 μM) [MacPherson et al., 1997] or the broad-spectrum metalloprotease inhibitors GM6001 (10 μM) [Hao et al., 1999] or TAPI-0 (50 μM) [Mohler et al., 1994]. Levels of soluble/shed BTC ectodomains in CM were detected by EIA using the anti-BTC ectodomain Asp^{32}–Tyr^{111} antibody (left). Results are expressed as mean ± SD of triplicate determinations. Lysates were collected from MB52 cells cultivated for 48 h in serum-free DMEM with or without DMSO (vehicle), GM6001 (50 μM), or TAPI-0 (50 μM) and the degree of pro-BTC ectodomain shedding analyzed by Western blot using the anti-BTC C-terminus Asp^{164}–Ala^{178} antibody.

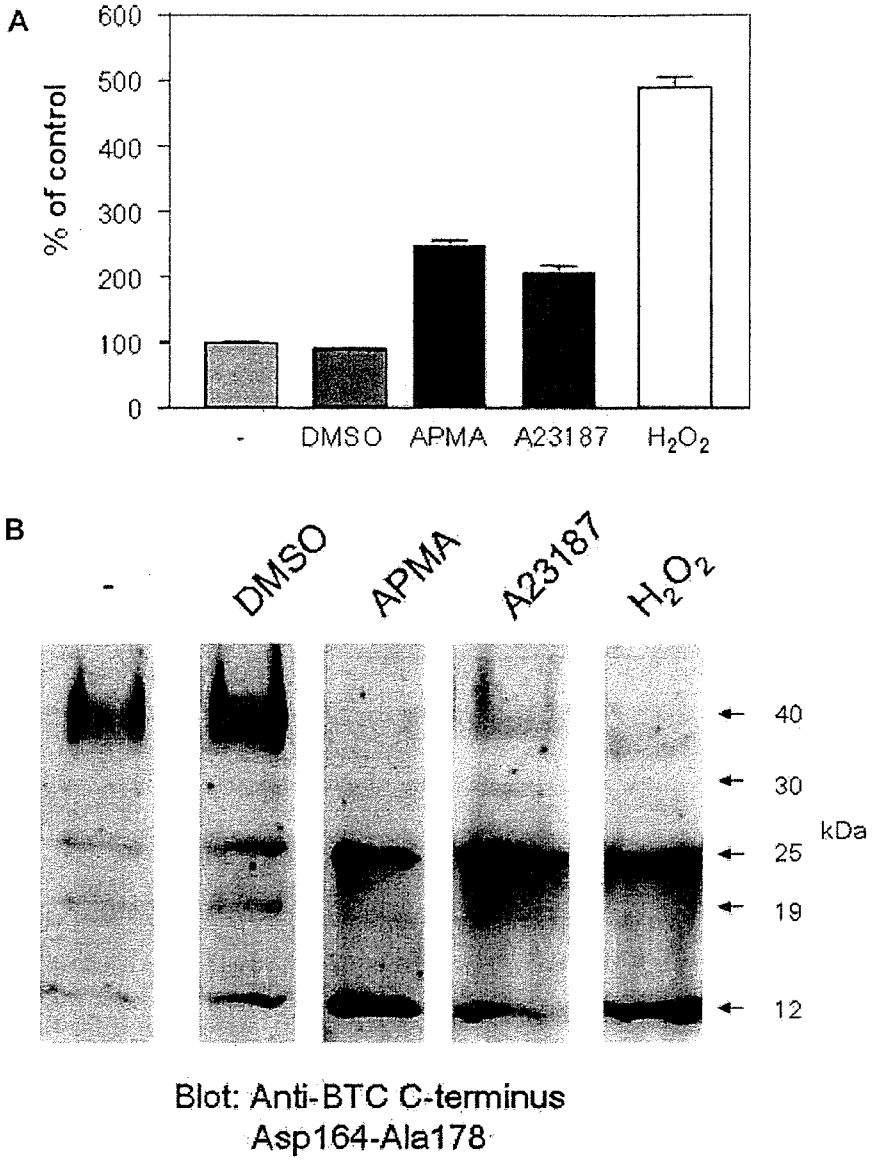

Fig. 2. The novel stimuli hydrogen peroxide activates pro-BTC shedding. **A:** MB52 cells were cultured in serum-free DMEM in the presence or absence of DMSO (vehicle), APMA (0.5 mM), A23187 (1 μM), or H_2O_2 (1 mM) for 4 h and then level of soluble/shed BTC in CM was detected by EIA using the anti-BTC ectodomain Asp^{32}–Tyr^{111} antibody. Results are expressed as the mean ± SD of triplicate determinations. **B:** Cell lysates from the treatment described in A were harvested and analyzed by Western blot using the anti-BTC C-terminus Asp^{164}–Ala^{178} antibody.

Asp^{164}–Ala^{178} antibody showed that the decrease in levels of the 40 kDa pro-BTC fragment, characteristic of activated pro-BTC shedding, in response to H_2O_2 was impaired in the presence of TAPI-0 (Fig. 3B).

The metalloprotease ADAM17 is responsible for ectodomain shedding of most EGF-like factors under constitutive and activated conditions [Sunnarborg et al., 2002; Sahin et al., 2004]. In addition, several studies have shown that ADAM17 is directly activated by ROS and subsequently mediates shedding of transmembrane molecules including TNFα and the TNF receptor [Hino et al., 1999; Zhang et al., 2001; Pietri et al., 2005]. We investigated the role of ADAM17 in H_2O_2-induced shedding of pro-BTC using conditionally immortalized stomach epithelial cells (STOM) from wild-type and $ADAM17^{\Delta Zn/\Delta Zn}$ mice transduced with a retroviral construct for expression of pro-BTC [Sanderson et al., 2005]. These STOM $ADAM17^{\Delta Zn/\Delta Zn}$ cells carry a targeted deletion in the catalytic

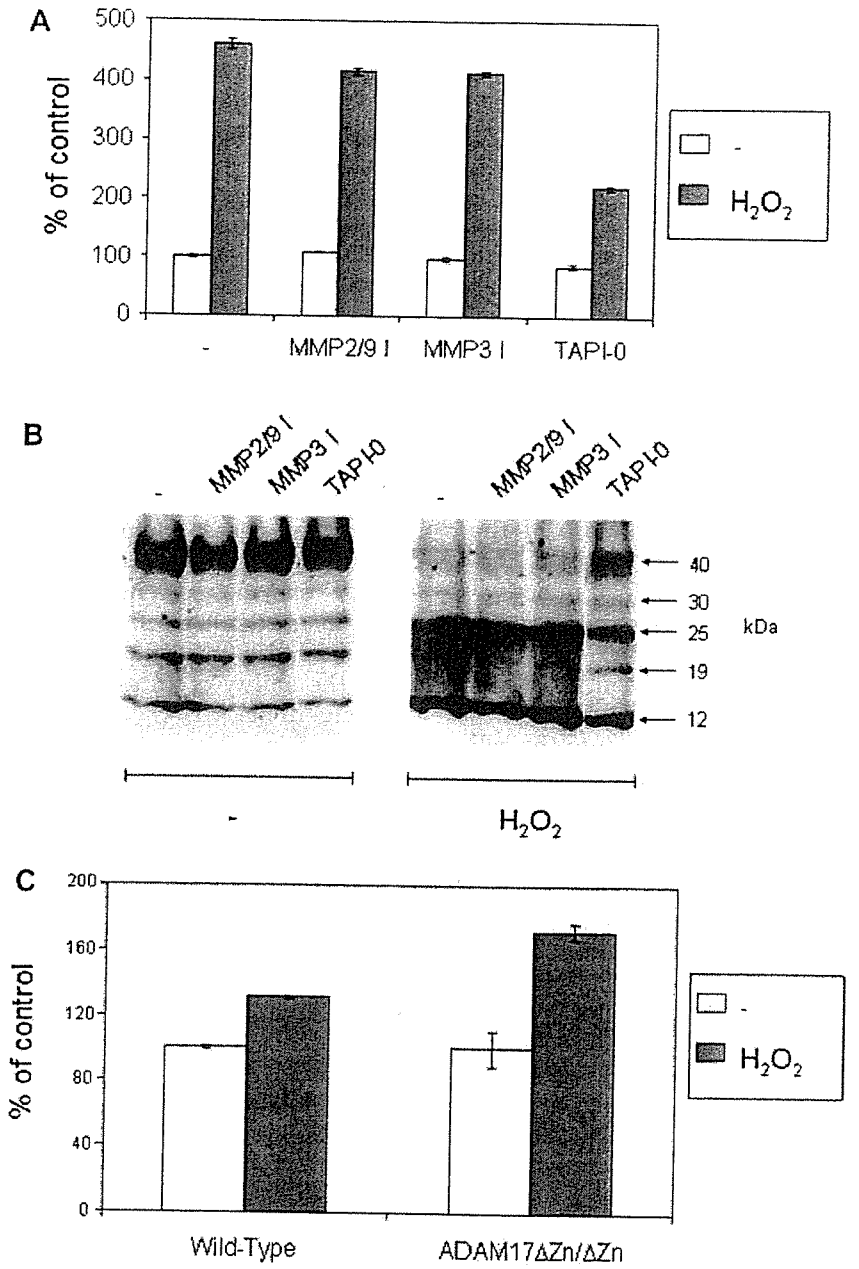

Fig. 3. H_2O_2-activation of pro-BTC shedding involves a metalloprotease other than ADAM17. **A:** MB52 cells were pre-incubated in serum-free DMEM with or without DMSO, MMP2/9 inhibitor (10 μM), MMP3 inhibitor (10 μM), or TAPI-0 (50 μM). The specificity of each of these inhibitors is described in the legend to Figure 1. The BTC-shedding activator H_2O_2 was then added directly to the culture media to a final concentration of 1 mM and cells cultured for a further 4 h. Levels of soluble/shed BTC in CM was determined using the BTC EIA with the anti-BTC ectodomain Asp^{32}–Tyr^{111} antibody. Results are expressed as the mean ± SD of triplicate determinations. **B:** Cell lysates from the treatment described in A were harvested and analyzed by Western blot using the anti-BTC C-terminus Asp^{164}–Ala^{178} antibody. **C:** STOM cells expressing pro-BTC from wild-type and $ADAM17^{\Delta Zn/\Delta Zn}$ mutant mice were cultured in serum-free DMEM with or without 100 μM H_2O_2 for 4 h. CM was collected and levels of shed/soluble BTC ectodomains measured using the BTC ELISA. Results are expressed as the mean ± SD of quadruplicate determinations.

zinc-binding domain of ADAM17 and have previously been used to directly link ADAM17 with the ectodomain shedding of transmembrane molecules such as VCAM-1 [Garton et al., 2003] and fractalkine (CX3CL1) [Garton et al., 2001]. Cells were treated with or without 100 μM H_2O_2 and then CM was collected. Due to the toxicity of 1 mM H_2O_2 towards STOM

cells, a lower dose of 100 μM was used. As a result of this sub-optimal dose, a lower induction of pro-BTC shedding of between 0.5- to 2-fold was generally observed (data not shown). H_2O_2-induced shedding of pro-BTC into CM was comparable between wild-type and ADAM17$^{\Delta Zn/\Delta Zn}$ cells (Fig. 3C). These results indicate that unlike a variety of other transmembrane molecules, pro-BTC is not a substrate for ADAM17 in response to H_2O_2 induction and that a separate metalloprotease such as ADAM10 is likely to be involved.

A23187 and H_2O_2 Activate Pro-BTC Shedding by Distinct Mechanisms

Despite an enormous amount of research into ectodomain shedding, a clear picture of the molecular mechanisms by which various chemical and physiological stimuli lead to activation of metalloproteases remains mostly uncharacterized. In the case of PMA-activated shedding, a link to PKC has been described [Pandiella and Massague, 1991], whereas for calcium-ionophore, calcium influx into the cell presumably activates calcium-dependent signaling pathways to induce shedding [Eguchi et al., 1998].

The requirement of extracellular calcium ions for H_2O_2-induced pro-BTC ectodomain shedding was investigated. MB52 cells were pre-incubated in DMEM or calcium-free DMEM, and then H_2O_2, A23187, or APMA added for 4 h. Western analysis of lysates, using the anti-BTC C-terminus Asp^{164}–Ala^{178} antibody, indicated that only the A23187-mediated decrease in levels of the 40 kDa pro-BTC isoform was impaired by culture in calcium-free media (Fig. 4A). This was consistent with our previous findings on the blockage of A23187-activated pro-BTC ectodomain shedding in calcium-free media [Sanderson et al., 2005].

In some cases, metalloprotease activation has been proposed to occur by oxidative removal of the enzymes pro-inhibitory region by a 'cysteine-switch mechanism' [Nagase and Woessner, 1999; Roghani et al., 1999]. Therefore, the ability of an anti-oxidant N-acetyl-L-cysteine to block H_2O_2-induced pro-BTC shedding was investigated. MB52 cells were pre-incubated in N-acetyl-L-cysteine for 30 min, and

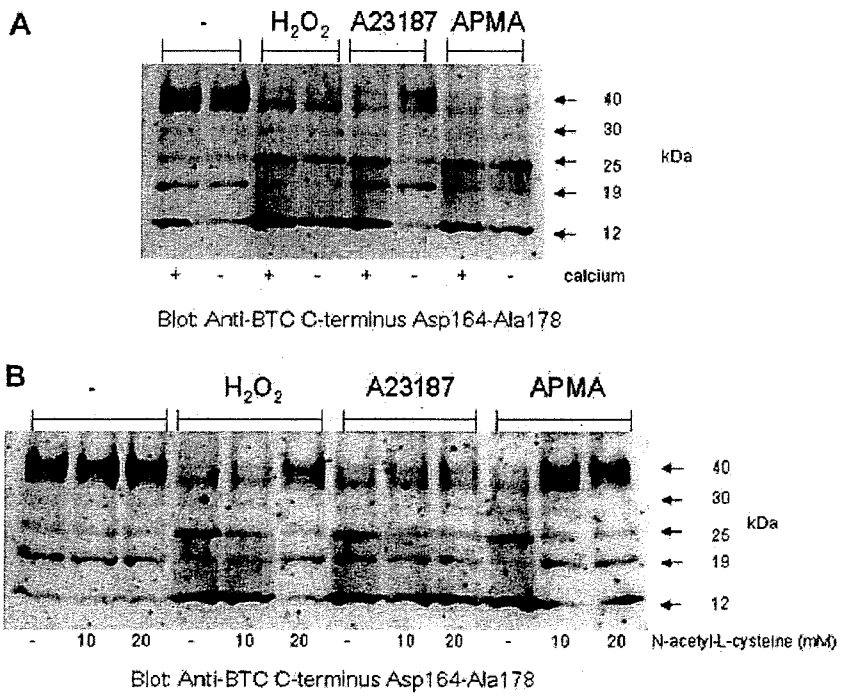

Fig. 4. A23187 and H_2O_2 activate pro-BTC shedding by distinct pathways. **A:** MB52 cells were pre-incubated in DMEM or calcium-free DMEM for 30 min, then the pro-BTC shedding activators H_2O_2 (1 mM), A23187 (1 μM), or APMA (0.5 mM) added and cells cultured for a further 4 h. The level of pro-BTC shedding was assessed by analysis of cell lysates by Western blot with the anti-BTC C-terminus Asp^{164}–Ala^{178} antibody. **B:** MB52 cells were pre-incubated in DMEM or N-acetyl-L-cysteine (10 or 20 mM) for 30 min, then H_2O_2 (1 mM), A23187 (1 μM), or APMA (0.5 mM) added and cells cultured for a further 4 h. Cell lysates were collected, and then analyzed by Western blot with the anti-BTC C-terminus Asp^{164}–Ala^{178} antibody.

then H_2O_2, A23187, or APMA were added for 4 h. Only activated pro-BTC shedding in response to H_2O_2 and APMA was impaired in the presence of N-acetyl-L-cysteine (Fig. 4B). A23187-activated shedding was unaffected by anti-oxidant treatment. These findings suggest H_2O_2 and APMA activate pro-BTC shedding via a calcium-independent/ROS-dependent mechanism whereas conversely A23187-activated pro-BTC shedding operates through a calcium-dependent/ROS-independent mechanism.

Endothelin-1 Activates the Metalloprotease-Dependent Shedding of BTC in Vascular Smooth Muscle Cells

A number of studies have indicated that GPCR agonists such as angiotensin II (AngII) [Eguchi et al., 2003], ET-1 [Iwasaki et al., 1998], l-α-lysophosphatidic acid (LPA) [Gschwind et al., 2003], and the glucagon-like peptide 1 (GLP-1) [Buteau et al., 2003] activate metalloprotease-dependent shedding of EGF-like factors. Therefore, the ability of GPCR agonists to stimulate pro-BTC shedding in primary VSMCs overexpressing pro-BTC was investigated. VSMCs have previously been demonstrated to shed other EGF-like factors, such as HB-EGF, in response to GPCR agonists [Mifune et al., 2004, 2005]. A number of GPCR agonists were tested but only ET-1 consistently stimulated pro-BTC shedding. This was blocked by preincubation with the broad-spectrum metalloprotease inhibitor GM6001 (Fig. 5A). Activation of pro-BTC shedding by ET-1 was consistently weaker than that by A23187.

ADAM10 and ADAM17 are Both Involved in ET-1-activated Pro-BTC Shedding in VSMCs

To investigate the role of ADAM10 and ADAM17 in ET-1-activated pro-BTC shedding, these enzymes were overexpressed in VSMCs expressing pro-BTC. Expression of ADAMs was confirmed by Western blot (data not shown). Wild-type ADAM10 overexpression enhanced ET-1-activated pro-BTC shedding (Fig. 5B), whereas overexpression of E385A catalytically inactive ADAM10 reduced the ET-1 effect. Interestingly, activation of shedding by ET-1 was also enhanced in cells overexpressing wild-type ADAM17; however, E406A ADAM17 was without effect. This may indicate that ET-1 can activate ADAM17 to shed pro-BTC, but that in a system of dysfunctional ADAM17 activity (i.e., E406A ADAM17 overexpression), ADAM10 may be sufficient for ET-1-activated pro-BTC shedding. Similar to our previously published data in conditionally immortalized dermal fibroblasts and STOM cells [Sanderson et al., 2005], A23187-activated and constitutive shedding of pro-BTC in VSMCs was reduced by overexpression of E385A ADAM10 and increased by wild-type ADAM10 expression, but was unaffected by ADAM17 or E406A ADAM17 overexpression (Fig. 5C).

DISCUSSION

Ectodomain shedding of EGF-like growth factors is an essential process that regulates the availability of soluble ErbB ligands. Like all other EGF-like factors, pro-BTC is expressed as a transmembrane precursor that undergoes ectodomain shedding to release a soluble mature factor from the cell surface [Sanderson et al., 2005]. In this study, MB52 cells shed detectable levels of BTC ectodomains into conditioned media (CM). Three BTC ectodomain isoforms were identified in MB52 CM using an anti-BTC ectodomain Asp^{32}–Tyr^{111} antibody. These forms have molecular masses similar to soluble BTC forms identified in conditionally immortalized cells and A9 mouse fibroblasts that vary in their N-terminal sequence and level of glycosylation [Watanabe et al., 1994; Sanderson et al., 2005]. Unlike in conditionally immortalized cells, in which pro-BTC shedding is highly preferred over N-terminal processing [Sanderson et al., 2005], MB52 cells appeared to mediate both cleavage events to a similar extent. This was highlighted by the equivalent accumulation of the 25 kDa pro-BTC form and 12 kDa cytoplasmic remnant in response to stimuli, and the predominant appearance of the 7 kDa shed BTC isoform in MB52 cell CM. Whilst the possibility that shed BTC forms are processed further once released into CM cannot be excluded, this alternate processing pattern may reflect an important distinction between the mechanisms of pro-BTC shedding between different cell lines, and possibly alternate regulation of sheddases.

Ectodomain shedding of EGF-like factors has been linked to metalloproteases of the ADAM and MMP families [Blobel, 1997]. In the case of BTC, constitutive and activated shedding is primarily dependent on ADAM10, and independent of ADAM17 [Hinkle et al., 2004; Sahin et al., 2004; Sanderson et al., 2005]. This

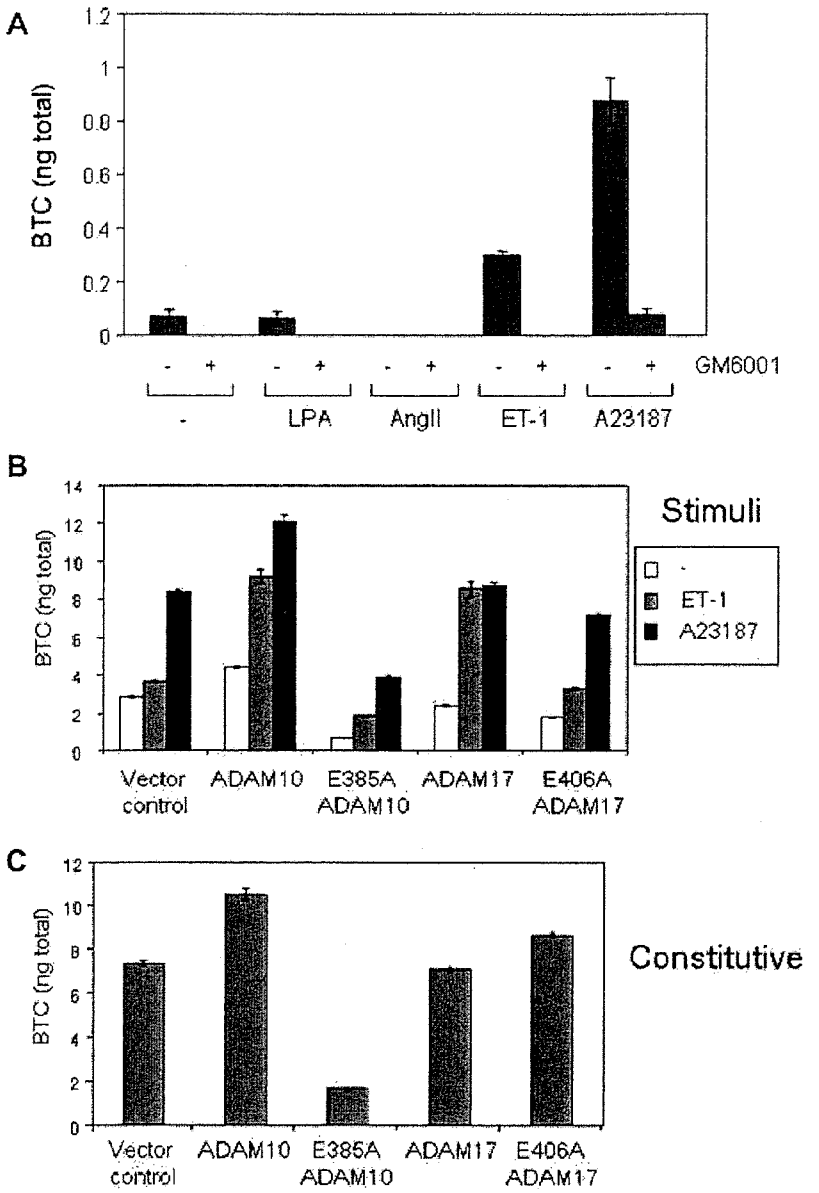

Fig. 5. Endothelin-1 activates ADAM10- and ADAM17-dependent pro-BTC shedding in vascular smooth muscle cells. **A:** VSMCs expressing pro-BTC were pre-incubated for 30 min in GM6001 (50 μM) and then treated for 1 h with LPA (10 μM), AngII (1 μM), or ET-1 (10 μM). CM was collected and analyzed for soluble/shed BTC levels using the BTC ELISA. Results are expressed as mean ± SD of quadruplicate determinations. **B:** VSMCs expressing pro-BTC and overexpressing wild-type and E > A forms of ADAM10 and ADAM17 were cultured and treated with ET-1 (10 μM) or A23187 (5 μM). CM was collected and analyzed for levels of soluble/shed BTC using the BTC ELISA. Results are expressed as mean ± SD of quadruplicate determinations. **C:** The same VSMC lines expressing the vector control or wild-type or E > A forms of ADAM10 and ADAM17 in B were cultured for 24 h in serum-free media to assess the level of constitutive pro-BTC shedding. Levels of BTC in CM were determined using the BTC ELISA as above.

distinguishes BTC from other EGF-like factors including TGFα [Peschon et al., 1998], NRG-1 [Montero et al., 2000], HB-EGF and AR [Sunnarborg et al., 2002], and ER [Hinkle et al., 2004; Sahin et al., 2004] which are predominantly ADAM17 substrates. Consistent with this, pro-BTC shedding is not up-regulated by PMA, which is a common activator of ADAM17-dependent shedding events [Nagano et al., 2004]. In this study, metalloprotease-dependent pro-BTC shedding in MB52 cells was activated by treatment with A23187, APMA and the novel stimuli H_2O_2. H_2O_2 was consistently the most powerful activator of pro-BTC shedding.

The activation of pro-BTC shedding by APMA and H_2O_2 was distinct from that involving A23187. Pre-incubation with anti-oxidant blocked APMA- and H_2O_2-induced, but not A23187-induced, pro-BTC shedding. Whereas A23187-induced, but not APMA- or H_2O_2-induced, shedding was attenuated when cells were deprived of extracellular calcium. Previous work has found that shedding of EGF-like ligands can be activated by multiple stimuli that operate by seemingly independent mechanisms [Pandiella and Massague, 1991]. The mechanism by which APMA/H_2O_2 and A23187 lead to activation of pro-BTC shedding presumably involves the activation of metalloproteases, yet how this eventuates is likely to be divergent. APMA- and H_2O_2-activated pro-BTC shedding most likely occurs by direct oxidative removal of the metalloprotease pro-peptide inhibitory region. MMPs and ADAMs contain an N-terminal inhibitory pro-peptide region that blocks the catalytic domain by a 'cysteine-switch mechanism' [Nagase and Woessner, 1999]. ROS have previously been shown to stimulate removal of the inhibitory pro-domain of ADAMs [Zhang et al., 2001], and in some cases lead to activation of ectodomain shedding [Hino et al., 1999]. The ability of N-acetyl-L-cysteine to block APMA- and H_2O_2-activated pro-BTC shedding most likely implicates this mechanism of metalloprotease activation.

Interestingly, the short vasoactive peptide ET-1 was the only GPCR agonist that activated pro-BTC shedding in VSMCs. ET-1 is expressed by epithelial, mesangial, neuronal, and liver cells [Levin, 1996] and mediates cellular effects such as proliferation and migration via binding of two separate GPCRs; ETA and ETB [Sokolovsky, 1995]. Binding of ET-1 to either ETA or ETB results in receptor coupling to multiple G-proteins (G_q, G_s, and G_i) [Eguchi et al., 1993] and subsequent signal transduction through numerous effectors including phospholipases C, D, and A2, as well as adenylate and guanylate cyclases and multiple kinases [Douglas and Ohlstein, 1997]. ETA and ETB receptors have also been linked with influx of extracellular calcium [Pollock et al., 1995] and generation of ROS [Daou and Srivastava, 2004], raising the possibility that activated pro-BTC shedding in response to A23187, APMA, or H_2O_2 may reflect a similar signaling mechanism to the activation of shedding by ET-1.

In contrast to constitutive and A23187-activated pro-BTC shedding in VSMCs, which mapped solely to ADAM10, activation of pro-BTC shedding by ET-1 was enhanced by overexpression of both ADAM10 and ADAM17. Only E385A ADAM10 expression reduced ET-1-activated pro-BTC shedding, suggesting the ADAM10 is the primary ET-1-activated pro-BTC sheddase. ET-1 has previously been shown to transactivate the ErbB1 receptor via metalloprotease-dependent shedding of EGF-like factors [Kawanabe et al., 2004]. However, the findings here provide the first evidence of ET-1-activation of ADAM10 and ADAM17 and also the first indication of an involvement of ET-1 in pro-BTC shedding. In addition this is the first cellular evidence that under certain conditions, ADAM17 may be involved in processing of pro-BTC.

Ectodomain shedding is potentially fundamental in the development of EGF-like factor-dependent tumors [Borrell-Pages et al., 2003] and other diseases [Sasada and Igarashi, 1993; Mifune et al., 2004] involving deregulated cell growth. Our results identify ROS and ET-1 as novel stimuli towards metalloprotease-dependent ectodomain shedding of pro-BTC. This provides direction for further analysis of the role of pro-BTC and physiological stimuli in the progression of such abnormalities in vivo.

ACKNOWLEDGMENTS

This work was supported in part by the Australian Government Cooperative Research Centers Programme to MP Sanderson CA Abbott and AJ Dunbar, and to PJ Dempsey by National Institute of Health (NIH) grants DK59778 and DK63363 and a grant from the Crohn's and Colitis Foundation of America. We thank GroPep Ltd for the use of research facilities, Roy Black and Jacques Peschon (Amgen) for providing ADAM17 reagents, Elaine Raines (University of Washington, Seattle, WA) for providing ADAM10 reagents, Garry Nolan (Stanford University) for providing the pBM retroviral vector, and Sarah Erickson and Sarah Fitzgerald (PNRI, Seattle, WA) for their excellent technical support.

REFERENCES

Blobel CP. 1997. Metalloprotease-disintegrins: Links to cell adhesion and cleavage of TNF alpha and Notch. Cell 90: 589–592.

Borrell-Pages M, Rojo F, Albanell J, Baselga J, Arribas J. 2003. TACE is required for the activation of the EGFR by TGF-alpha in tumors. Embo J 22:1114–1124.

Buteau J, Foisy S, Joly E, Prentki M. 2003. Glucagon-like peptide 1 induces pancreatic beta-cell proliferation via transactivation of the epidermal growth factor receptor. Diabetes 52:124–132.

Daou GB, Srivastava AK. 2004. Reactive oxygen species mediate endothelin-1-induced activation of ERK1/2, PKB, and Pyk2 signaling, as well as protein synthesis, in vascular smooth muscle cells. Free Radic Biol Med 37: 208–215.

Del Giudice G, Pizza M, Rappuoli R. 1998. Molecular basis of vaccination. Mol Aspects Med 19:1–70.

Douglas SA, Ohlstein EH. 1997. Signal transduction mechanisms mediating the vascular actions of endothelin. J Vasc Res 34:152–164.

Dunbar AJ, Goddard C. 2000. Structure-function and biological role of betacellulin. Int J Biochem Cell Biol 32:805–815.

Eguchi S, Hirata Y, Imai T, Marumo F. 1993. Endothelin receptor subtypes are coupled to adenylate cyclase via different guanyl nucleotide-binding proteins in vasculature. Endocrinology 132:524–529.

Eguchi S, Numaguchi K, Iwasaki H, Matsumoto T, Yamakawa T, Utsunomiya H, Motley ED, Kawakatsu H, Owada KM, Hirata Y, Marumo F, Inagami T. 1998. Calcium-dependent epidermal growth factor receptor transactivation mediates the angiotensin II-induced mitogen-activated protein kinase activation in vascular smooth muscle cells. J Biol Chem 273:8890–8896.

Eguchi S, Frank GD, Mifune M, Inagami T. 2003. Metalloprotease-dependent ErbB ligand shedding in mediating EGFR transactivation and vascular remodelling. Biochem Soc Trans 31:1198–1202.

Fischer OM, Hart S, Gschwind A, Ullrich A. 2003. EGFR signal transactivation in cancer cells. Biochem Soc Trans 31:1203–1208.

Garton KJ, Gough PJ, Blobel CP, Murphy G, Greaves DR, Dempsey PJ, Raines EW. 2001. Tumor necrosis factor-alpha-converting enzyme (ADAM17) mediates the cleavage and shedding of fractalkine (CX3CL1). J Biol Chem 276:37993–38001.

Garton KJ, Gough PJ, Philalay J, Wille PT, Blobel CP, Whitehead RH, Dempsey PJ, Raines EW. 2003. Stimulated shedding of vascular cell adhesion molecule 1 (VCAM-1) is mediated by tumor necrosis factor-alpha-converting enzyme (ADAM 17). J Biol Chem 278:37459–37464.

Gechtman Z, Alonso JL, Raab G, Ingber DE, Klagsbrun M. 1999. The shedding of membrane-anchored heparin-binding epidermal-like growth factor is regulated by the Raf/mitogen-activated protein kinase cascade and by cell adhesion and spreading. J Biol Chem 274:28828–28835.

Gschwind A, Hart S, Fischer OM, Ullrich A. 2003. TACE cleavage of proamphiregulin regulates GPCR-induced proliferation and motility of cancer cells. Embo J 22: 2411–2421.

Hao JL, Nagano T, Nakamura M, Kumagai N, Mishima H, Nishida T. 1999. Galardin inhibits collagen degradation by rabbit keratocytes by inhibiting the activation of pro-matrix metalloproteinases. Exp Eye Res 68:565–572.

Hao L, Du M, Lopez-Campistrous A, Fernandez-Patron C. 2004. Agonist-induced activation of matrix metalloproteinase-7 promotes vasoconstriction through the epidermal growth factor-receptor pathway. Circ Res 94:68–76.

Higashiyama S. 2004. Metalloproteinase-mediated shedding of heparin-binding EGF-like growth factor and its pathophysiological roles. Protein Pept Lett 11:443–450.

Hinkle CL, Sunnarborg SW, Loiselle D, Parker CE, Stevenson M, Russell WE, Lee DC. 2004. Selective roles for tumor necrosis factor alpha-converting enzyme/ADAM17 in the shedding of the epidermal growth factor receptor ligand family: The juxtamembrane stalk determines cleavage efficiency. J Biol Chem 279:24179–24188.

Hino T, Nakamura H, Abe S, Saito H, Inage M, Terashita K, Kato S, Tomoike H. 1999. Hydrogen peroxide enhances shedding of type I soluble tumor necrosis factor receptor from pulmonary epithelial cells. Am J Respir Cell Mol Biol 20:122–128.

Horiuchi K, Zhou HM, Kelly K, Manova K, Blobel CP. 2005. Evaluation of the contributions of ADAMs 9, 12, 15, 17, and 19 to heart development and ectodomain shedding of neuregulins beta1 and beta2. Dev Biol 283:459–471.

Ino K, Nagasaka T, Okamoto T, Uehara C, Nakazato H, Nakashima N, Mizutani S. 2000. Expression of aminopeptidase A in human gestational choriocarcinoma cell lines and tissues. Placenta 21:63–72.

Iwasaki H, Eguchi S, Marumo F, Hirata Y. 1998. Endothelin-1 stimulates DNA synthesis of vascular smooth-muscle cells through transactivation of epidermal growth factor receptor. J Cardiovasc Pharmacol 31 Suppl 1:S182–S184.

Kawanabe Y, Masaki T, Hashimoto N. 2004. Involvement of epidermal growth factor receptor-protein tyrosine kinase transactivation in endothelin-1-induced vascular contraction. J Neurosurg 100:1066–1071.

Lautrette A, Li S, Alili R, Sunnarborg SW, Burtin M, Lee DC, Friedlander G, Terzi F. 2005. Angiotensin II and EGF receptor cross-talk in chronic kidney diseases: A new therapeutic approach. Nat Med 11:867–874.

Le Gall S, Auger R, Dreux C, Mauduit P. 2003. Regulated cell surface proEGF ectodomain shedding is a zinc-metalloprotease dependent process. J Biol Chem 278: 45255–45268.

Lemjabbar H, Basbaum C. 2002. Platelet-activating factor receptor and ADAM10 mediate responses to Staphylococcus aureus in epithelial cells. Nat Med 8:41–46.

Levin ER. 1996. Endothelins as cardiovascular peptides. Am J Nephrol 16:246–251.

Li Q, Park PW, Wilson CL, Parks WC. 2002. Matrilysin shedding of syndecan-1 regulates chemokine mobilization and transepithelial efflux of neutrophils in acute lung injury. Cell 111:635–646.

MacPherson LJ, Bayburt EK, Capparelli MP, Carroll BJ, Goldstein R, Justice MR, Zhu L, Hu S, Melton RA, Fryer L, Goldberg RL, Doughty JR, Spirito S, Blancuzzi V, Wilson D, O'Byrne EM, Ganu V, Parker DT. 1997. Discovery of CGS 27023A, a non-peptidic, potent, and orally active stromelysin inhibitor that blocks cartilage degradation in rabbits. J Med Chem 40:2525–2532.

McConnell RM, York JL, Frizzell D, Ezell C. 1993. Inhibition studies of some serine and thiol proteinases by new leupeptin analogues. J Med Chem 36:1084–1089.

Merlos-Suarez A, Ruiz-Paz S, Baselga J, Arribas J. 2001. Metalloprotease-dependent protransforming growth factor-alpha ectodomain shedding in the absence of tumor

necrosis factor-alpha-converting enzyme. J Biol Chem 276:48510–48517.

Mifune M, Ohtsu H, Suzuki H, Frank GD, Inagami T, Utsunomiya H, Dempsey PJ, Eguchi S. 2004. Signal transduction of betacellulin in growth and migration of vascular smooth muscle cells. Am J Physiol Cell Physiol 287:C807–C813.

Mifune M, Ohtsu H, Suzuki H, Nakashima H, Brailoiu E, Dun NJ, Frank GD, Inagami T, Higashiyama S, Thomas WG, Eckhart AD, Dempsey PJ, Eguchi S. 2005. G protein coupling and second messenger generation are indispensable for metalloprotease-dependent, heparin-binding epidermal growth factor shedding through angiotensin II type-1 receptor. J Biol Chem 280:26592–26599.

Mohler KM, Sleath PR, Fitzner JN, Cerretti DP, Alderson M, Kerwar SS, Torrance DS, Otten-Evans C, Greenstreet T, Weerawarna K, et al. 1994. Protection against a lethal dose of endotoxin by an inhibitor of tumour necrosis factor processing. Nature 370:218–220.

Montero JC, Yuste L, Diaz-Rodriguez E, Esparis-Ogando A, Pandiella A. 2000. Differential shedding of transmembrane neuregulin isoforms by the tumor necrosis factor-alpha-converting enzyme. Mol Cell Neurosci 16: 631–648.

Nagano O, Murakami D, Hartmann D, De Strooper B, Saftig P, Iwatsubo T, Nakajima M, Shinohara M, Saya H. 2004. Cell-matrix interaction via CD44 is independently regulated by different metalloproteinases activated in response to extracellular Ca2+ influx and PKC activation. J Cell Biol 165:893–902.

Nagase H, Woessner JF, Jr. 1999. Matrix metalloproteinases. J Biol Chem 274:21491–21494.

Olayioye MA, Neve RM, Lane HA, Hynes NE. 2000. The ErbB signaling network: Receptor heterodimerization in development and cancer. Embo J 19:3159–3167.

Pandiella A, Massague J. 1991. Multiple signals activate cleavage of the membrane transforming growth factor-alpha precursor. J Biol Chem 266:5769–5773.

Peschon JJ, Slack JL, Reddy P, Stocking KL, Sunnarborg SW, Lee DC, Russell WE, Castner BJ, Johnson RS, Fitzner JN, Boyce RW, Nelson N, Kozlosky CJ, Wolfson MF, Rauch CT, Cerretti DP, Paxton RJ, March CJ, Black RA. 1998. An essential role for ectodomain shedding in mammalian development. Science 282:1281–1284.

Pietri M, Schneider B, Mouillet-Richard S, Ermonval M, Mutel V, Launay JM, Kellermann O. 2005. Reactive oxygen species-dependent TNF-alpha converting enzyme activation through stimulation of 5-HT2B and alpha1D autoreceptors in neuronal cells. Faseb J 19:1078–1087.

Pollock DM, Keith TL, Highsmith RF. 1995. Endothelin receptors and calcium signaling. Faseb J 9:1196–1204.

Prenzel N, Zwick E, Daub H, Leserer M, Abraham R, Wallasch C, Ullrich A. 1999. EGF receptor transactivation by G-protein-coupled receptors requires metalloproteinase cleavage of proHB-EGF. Nature 402:884–888.

Richter A, O'Donnell RA, Powell RM, Sanders MW, Holgate ST, Djukanovic R, Davies DE. 2002. Autocrine ligands for the epidermal growth factor receptor mediate interleukin-8 release from bronchial epithelial cells in response to cigarette smoke. Am J Respir Cell Mol Biol 27:85–90.

Roghani M, Becherer JD, Moss ML, Atherton RE, Erdjument-Bromage H, Arribas J, Blackburn RK, Weskamp G, Tempst P, Blobel CP. 1999. Metalloprotease-disintegrin MDC9: Intracellular maturation and catalytic activity. J Biol Chem 274:3531–3540.

Sahin U, Weskamp G, Kelly K, Zhou HM, Higashiyama S, Peschon J, Hartmann D, Saftig P, Blobel CP. 2004. Distinct roles for ADAM10 and ADAM17 in ectodomain shedding of six EGFR ligands. J Cell Biol 164:769–779.

Sanderson MP, Erickson SN, Gough PJ, Garton KJ, Wille PT, Raines EW, Dunbar AJ, Dempsey PJ. 2005. ADAM10 mediates ectodomain shedding of the betacellulin precursor activated by p-aminophenylmercuric acetate and extracellular calcium influx. J Biol Chem 280:1826–1837.

Sasada R, Igarashi K. 1993. Betacellulin: A new growth factor for vascular smooth muscle cells. Nippon Rinsho 51:3308–3317.

Schlondorff J, Lum L, Blobel CP. 2001. Biochemical and pharmacological criteria define two shedding activities for TRANCE/OPGL that are distinct from the tumor necrosis factor alpha convertase. J Biol Chem 276: 14665–14674.

Scornik OA, Botbol V. 2001. Bestatin as an experimental tool in mammals. Curr Drug Metab 2:67–85.

Shing Y, Christofori G, Hanahan D, Ono Y, Sasada R, Igarashi K, Folkman J. 1993. Betacellulin: A mitogen from pancreatic beta cell tumors. Science 259:1604–1607.

Slupphaug G, Kavli B, Krokan HE. 2003. The interacting pathways for prevention and repair of oxidative DNA damage. Mutat Res 531:231–251.

Sokolovsky M. 1995. Endothelin receptor subtypes and their role in transmembrane signaling mechanisms. Pharmacol Ther 68:435–471.

Sunnarborg SW, Hinkle CL, Stevenson M, Russell WE, Raska CS, Peschon JJ, Castner BJ, Gerhart MJ, Paxton RJ, Black RA, Lee DC. 2002. Tumor necrosis factor-alpha converting enzyme (TACE) regulates epidermal growth factor receptor ligand availability. J Biol Chem 277: 12838–12845.

Tada H, Sasada R, Kawaguchi Y, Kojima I, Gullick WJ, Salomon DS, Igarashi K, Seno M, Yamada H. 1999. Processing and juxtacrine activity of membrane-anchored betacellulin. J Cell Biochem 72:423–434.

Takenobu H, Yamazaki A, Hirata M, Umata T, Mekada E. 2003. The stress- and inflammatory cytokine-induced ectodomain shedding of heparin-binding epidermal growth factor-like growth factor is mediated by p38 MAPK, distinct from the 12-O-tetradecanoylphorbol-13-acetate- and lysophosphatidic acid-induced signaling cascades. J Biol Chem 278:17255–17262.

Tamura Y, Watanabe F, Nakatani T, Yasui K, Fuji M, Komurasaki T, Tsuzuki H, Maekawa R, Yoshioka T, Kawada K, Sugita K, Ohtani M. 1998. Highly selective and orally active inhibitors of type IV collagenase (MMP-9 and MMP-2): N-sulfonylamino acid derivatives. J Med Chem 41:640–649.

Tanida S, Joh T, Itoh K, Kataoka H, Sasaki M, Ohara H, Nakazawa T, Nomura T, Kinugasa Y, Ohmoto H, Ishiguro H, Yoshino K, Higashiyama S, Itoh M. 2004. The mechanism of cleavage of EGFR ligands induced by inflammatory cytokines in gastric cancer cells. Gastroenterology 127:559–569.

Touyz RM. 2003. Reactive oxygen species in vascular biology: Role in arterial hypertension. Expert Rev Cardiovasc Ther 1:91–106.

Touyz RM, Yao G, Viel E, Amiri F, Schiffrin EL. 2004. Angiotensin II and endothelin-1 regulate MAP kinases through different redox-dependent mechanisms in human vascular smooth muscle cells. J Hypertens 22: 1141–1149.

Trautschold I, Werle E, Zickgraf-Rudel G. 1966. [On the kallikrein-trypsin-inhibitor]. Arzneimittelforschung 16: 1507–1515.

Ushio-Fukai M, Alexander RW. 2004. Reactive oxygen species as mediators of angiogenesis signaling: Role of NAD(P)H oxidase. Mol Cell Biochem 264:85–97.

Watanabe T, Shintani A, Nakata M, Shing Y, Folkman J, Igarashi K, Sasada R. 1994. Recombinant human betacellulin. Molecular structure, biological activities, and receptor interaction. J Biol Chem 269:9966–9973.

Wetzker R, Bohmer FD. 2003. Transactivation joins multiple tracks to the ERK/MAPK cascade. Nat Rev Mol Cell Biol 4:651–657.

Xu KP, Ding Y, Ling J, Dong Z, Yu FS. 2004. Wound-induced HB-EGF ectodomain shedding and EGFR activation in corneal epithelial cells. Invest Ophthalmol Vis Sci 45:813–820.

Zhang Z, Oliver P, Lancaster JJ, Schwarzenberger PO, Joshi MS, Cork J, Kolls JK. 2001. Reactive oxygen species mediate tumor necrosis factor alpha-converting, enzyme-dependent ectodomain shedding induced by phorbol myristate acetate. Faseb J 15:303–305.

Zhang J, Li H, Wang J, Dong Z, Mian S, Yu FS. 2004. Role of EGFR transactivation in preventing apoptosis in Pseudomonas aeruginosa-infected human corneal epithelial cells. Invest Ophthalmol Vis Sci 45:2569–2576.

ANTICANCER RESEARCH 26: xxx-xxx (2006)

No: 6682-H
Please mark the appropriate section for this paper
☐ Experimental
☐ Clinical
☐ Epidemiological

Mechanisms of the Growth-inhibitory Effect of the RNase-EGF Fused Protein Against EGFR-overexpressing Cells

SOJUN HOSHIMOTO[1], MASAKAZU UEDA[1], HIROMITSU JINNO[1], MASAKI KITAJIMA[1], JUNICHIRO FUTAMI[2] and MASAHARU SENO[2]

[1]*Depatment of Surgery, Keio University School of Medicine, 35 Shinanomachi, Shinjuku-ku, Tokyo 160-8582;*
[2]*Department of Bioscience and Biotechnology, Faculty of Engineering, Okayama University, Tsushima-naka, Okayama 700-8530, Japan*

Abstract. *Background: We previously showed the usefulness of a fused protein of human pancreatic ribonuclease1 (hRNase1) with human epidermal growth factor (hEGF) for molecular targeting of EGF receptor (EGFR)-overexpressing cells. In this study, the mechanisms underlying the inhibition of cell growth by RNase-EGF fused proteins was confirmed. Materials and Methods: Des.1-7 hRNase1 was genetically fused to hEGF. The fused proteins were expressed and isolated from Escherichia coli. The internalization of hRNase1-hEGF was confirmed by confocal fluorescence microscopy. The growth-inhibitory effect of the fused proteins was evaluated by MTT assay. Results: FITC-labelled hRNase1-hEGF was internalized into EGFR-overexpressing A431 cells. The internalization was not observed in A431 cells pre-treated with hEGF and EGFR-deficient H69 cells. The growth-inhibitory effect of des.1-7 hRNase1-hEGF against A431 cells was statistically significantly more pronounced than that of hRNase1-hEGF. Conclusion: RNase-EGF fused proteins are internalized through EGFR and inhibit cell growth by exerting their ribonucleolytic activity in the cytosol.*

High levels of expression of epidermal growth factor receptor (EGFR) and its ligands are common in several types of cancers, including esophageal cancer, breast cancer, non-small cell lung cancer and ovarian cancer, and have been demonstrated to be correlated with more aggressive disease, resistance to conventional chemotherapy and a poor prognosis (1-4). Therefore, patients with malignancies overexpressing EGFR need aggressive multidisciplinary treatment. Recent research has led to the development of a new generation of therapeutic strategies targeting specific molecular processes that promote tumor growth and survival. EGFR is one of the most promising candidates as a molecular target in anticancer therapy.

EGFR is a 170-kDa transmembrane glycoprotein with tyrosine kinase activity that is stimulated by the binding of growth factors, such as transforming growth factor (TGF)-α or epidermal growth factor (EGF), to the extracellular domain of the receptor (5). Ligand-binding induces the receptors to dimerize and activates the intracellular kinase domain present on each receptor, resulting in autophosphorylation at the tyrosine residues in the intracellular domain. The phosphorylated tyrosine residues activate downstream signaling pathways which regulate gene transcription and cell cycle progression (5, 6). Therefore a number of anti-EGFR strategies have been examined. Gefitinib (Iressa®; AstraZeneca Pharmaceuticals, Wilmington, DE, USA), a selective EGFR tyrosine kinase inhibitor, which blocks signal transduction by inhibiting the intrinsic kinase activity of EGFR (7), and cetuximab (Erbitax®; Bristol-Myers Sqibb Company, Princeton, NJ, USA), which is a chimeric monoclonal antibody that specifically binds to EGFR to prevent ligand-EGFR interaction (8), have been developed for clinical use.

Ligand-toxin conjugates called "immunotoxins" have been produced by using plant or bacterial toxins, such as ricin A contained in the castor bean plant, and *Pseudomonas* exotoxin (9). We have demonstrated that anti-EGFR monoclonal antibodies (B4G7) chemically conjugated to gelonin, a plant toxin of the ricin family, are specifically cytotoxic against EGFR-overproducing cells (10). However, they have not yet come to the stage of clinical application because of their non-specific toxicity against normal cells and their immunogenicity (11, 12). In an attempt to make immunotoxins safer for clinical use, we and others have explored the use of mammalian ribonuclease (RNase) instead of plant or bacterial toxins (13, 14).

Correspondence to: Masakazu Ueda, Department of Surgery, Keio University School of Medicine, 35 Shinanomachi, Shinjuku-ku, Tokyo 160-8582, Japan. Tel: 81-3-3353-1211, Fax: 81-3-3355-4707, e-mail: m_ueda@sc.itc.keio.ac.jp

Key Words: Ribonuclease, EGF receptor, targeting, internalization.

0250-7005/2006 $2.00+.40

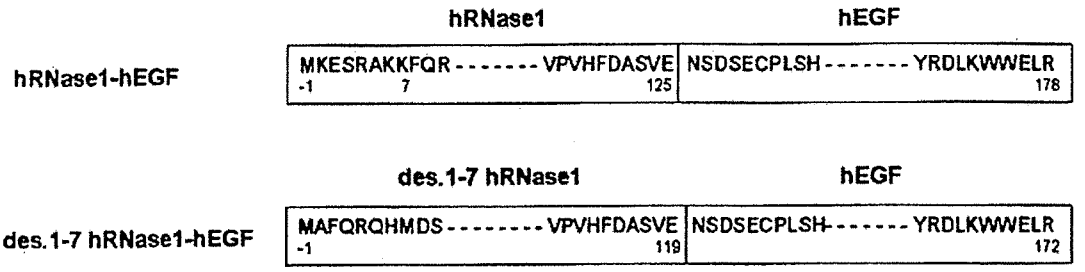

Figure 1. *Schematic representations of the fused proteins. Des.1-7 hRNase1 is constructed by truncating seven N-terminal amino acids from hRNase1. The C-terminal Glu of hRNase1 and des.1-7 hRNase1 are fused to the N-terminal Asn of hEGF.*

The RNase A superfamily consists of several extracellular enzymes with cytotoxic activity in addition to ribonucleolytic activity. Bovine seminal RNase and amphibian RNase (Onconase) have been shown to exert exceptional cytotoxic activity when added to the media of cell cultures (15, 16). The cytotoxic effects of these two RNases have been attributed to their internalization by nonreceptor-mediated endocytosis and their resistance to the inhibitory actions of the cytosolic RNase inhibitor. Most of the human RNases and bovine pancreatic RNase A are not cytotoxic by themselves, since they cannot enter the cytosol. However, these RNases were shown to inhibit protein synthesis when injected into *Xenopus* oocytes (17). Bovine pancreatic RNase A was chemically conjugated to human transferrin and to antibodies to the transferrin receptor (13). These conjugates were shown to exert cytotoxicity against cells bearing transferrin receptors. We previously demonstrated the cytotoxic effect of new immunotoxins exclusively constructed using endogenous proteins, *e.g.*, human pancreatic ribonuclease 1 (hRNase1) chemically conjugated or genetically fused to human EGF (hEGF), against EGFR-overexpressing cells (18, 19). However, two problems remained: first, internalization of the chemical conjugates or genetically fused proteins had not yet been identified directly and, second, we had not established conclusively that the cytotoxic effect of these agents was attributable to their RNase activity.

The intracellular RNase inhibitor, which binds and inactivates RNases, plays an important role in the protection of intrinsic RNA. In an attempt to reduce the affinity of RNases to the RNase inhibitor, we prepared des.1-7 hRNase1, with truncation of 7 amino acid residues in the amino-terminal sequence of hRNase1, which resulted in marked reduction of the RNase activity, but also in a significantly more pronounced reduction in the binding affinity to human placental RNase inhibitor (20). In the present study, we attempted to visualize the internalization of the fused proteins into cancer cells through the EGFR, and also to determine the contribution of the RNase activity of the fused protein in the cytosol to its growth-inhibitory effect, by comparing the cytotoxic effects of genetically fused hRNase1-hEGF and des.1-7 hRNase1-hEGF against EGFR-overexpressing cells.

Materials and Methods

Materials. The plasmid pRNEGF1, which is the expression plasmid constructed by inserting DNA fragments encoding hRNase1 and hEGF into a pET30b(+) expression vector with N-terminal XbaI and C-terminal BamHI sites, was purified from *Escherichia coli*, as described previously (19). The plasmid pBO54, derived from the pET8c expression vector, carries the gene for des.1-7 hRNase1 (20). The plasmid pADH59, an expression vector for hEGF, was purchased from the American Type Culture Collection. The T7 expression vector pET28a(+) and *E.coli* BL21(DE3)/pLysS were purchased from Novagen (Madison, WI, USA).

Cell lines. The A431 human vulvar carcinoma cell line overexpressiing EGFR and an H69 small cell lung carcinoma cell line with undetectable EGFR expression were obtained from the Japanese Cancer Research Resources Bank. A431 was grown in Dulbecco's modified Eagle's medium (DMEM), supplemented with 10% fetal calf serum, 1 mg/ml amphotericin B and 100 μg/ml kanamycin, while H69 was grown in RPMI 1640 containing the same supplements. Both the cell lines were cultured in a humidified atmosphere of 5% CO_2 in air at 37°C. The EGFR number determination in each cell line was performed as described previously (14).

Plasmid construction of des.1-7 hRNase1-hEGF. The plasmid pBO54 was used to create the C-terminal EcoRI restriction site at the codon for Glu119 of des.1-7 hRNase1 (reviewed in ref.(21); Figure 1B) by site-directed mutagenesis, and digested with NcoI and EcoRI to isolate the DNA fragment of des.1-7 hRNase1. The plasmid pADH59 was used to create the N-terminal EcoRI site at the codon for Asn1 of hEGF by PCR mutagenesis. The PCR products were digested with N-terminal EcoRI sites and C-terminal SalI sites which are attached after two stop codons in pADH59, to isolate the DNA fragment of hEGF. Both of the DNA fragments were ligated at the C-terminus of des.1-7 hRNase1 and N-terminus of hEGF without any additional amino acids or spacers (Figure 1), and inserted into the multiple cloning site of the expression vector pET28a(+) with NcoI and SalI sites. The expression plasmids of the two fused proteins, hRNase1-hEGF and des.1-7 hRNase1-hEGF, were subsequently transformed into the expression host BL21(DE3)/pLysS.

*Expression of hRNase1-EGF and des.*1-7 RNase1-EGF in *E.coli*. Expression cultures were grown at 37°C in TB medium supplemented with 30 μg/ml of kanamycin until the absorbance at 600 nm reached 1.0. Isopropyl-1-β-D-thiogalactopyranoside (IPTG) was then added to a final concentration of 0.5 mM, and the cultures were continued for a further 3 h at 37°C. The cells were harvested by centrifugation at 4°C and stored at –80°C until the purification steps.

Purification of hRNase1-EGF and des.1-7 RNase1-EGF. The frozen cell pellets from 1 l of the culture medium were thawed at 37°C and suspended in 15 ml of 10 mM Tris-HCl buffer, pH 7.5, containing 0.2 M NaCl, 10 mM $MgCl_2$ and 20% (w/v) sucrose. The suspensions were sonicated and homogenized, followed by the addition of 5 μg/ml each of DNase and RNase. Insoluble fractions containing recombinant proteins were precipitated by centrifugation at 12000 x g for 10 min at 4°C. The precipitates were dissolved in 10 ml of a denaturing buffer consisting of 0.1 M Tris-HCl, pH 8.0, and 6 M guanidine hydrochloride, and reduced with 0.1 M mercaptoethanol. The denatured and reduced proteins were subsequently refolded by rapid dilution into a refolding buffer consisting of 20 mM Tris-HCl, pH 8.0, 0.4 M guanidine hydrochloride, 30% (v/v) glycerol, 0.5 mM oxidized glutathione and 2 mM reduced glutathione/mercaptoethanol, at room temperature for 24 h. The supernatants were applied to columns filled with CM-Toyopearl 650C (Tosoh, Tokyo, Japan) and the folded proteins were eluted with 20 ml of 50 mM sodium acetate, pH 5.0, containing 0.5 M NaCl. The fused proteins were diluted 5-fold with distilled water and purified by cation-exchange chromatography on a HiTrap™ SP column (Amersham Biosciences, Piscataway, NJ, USA) with graded concentrations of NaCl in 50 mM sodium acetate buffer, pH 5.0. The fused proteins were desalted and concentrated using Amicon® Ultra-15 Centrifugal Filter (Millipore, Billerica, MA, USA) before the analysis.

The amino acid compositions of the fused proteins were determined in a Hitachi (Tokyo, Japan) L8800 amino acid analyzer, and the N-terminal sequence of the fused proteins were determined with an Applied Biosystems (Foster City, CA, USA) Procise™ 491 protein sequencer.

Enzyme assay. The RNase activity of each of the recombinant proteins was determined using yeast tRNA as the substrate. The assays were performed at pH 7.5, in accordance with a previously described protocol (22).

Preparation of fluorescence-labelled proteins. To visualize their specific binding to the cellular surface and the receptor-mediated cellular uptake, hRNase1-hEGF and holo-transferrin (Sigma, St. Louis, MO, USA) ligands were labelled with either fluorescein-isothiocyanate (FITC; Wako Chemical, Osaka, Japan) or rhodamine B isothiocyanate (RITC; Sigma). Each protein was incubated with an 8-molar excess amount of FITC or RITC in 80 mM sodium borate buffer, pH 8.5, for 2 h at room temperature. The labelled proteins thus obtained using the PD-10 column (Amersham Biosciences) were extracted using phosphate-buffered saline (PBS) as the elution buffer.

Fluorescence-microscopic analysis. To analyze the specific binding of FITC-hRNase1-hEGF to A431 cells, the cells were made to adhere to a cover slip (16 mm diameter) in DMEM supplemented with 10% fetal bovine serum (FBS) for 24 h. After washing once with DMEM, the cells were incubated with 300 nM of FITC-hRNase1-EGF, in the presence (2%) or absence of FBS, for 18 h or 30 min, respectively. Then, after washing twice with PBS, the fluorescence images were directly examined under a confocal laser-scanning microscope (Zeiss LSM-510 META; Carl Zeiss, Oberkochen, Germany) without fixation. For the competition assay, the cells were pre-incubated with 10 μM of EGF (Sigma) for 5 min, and then treated with 300 nM of FITC-hRNase1-hEGF. To confirm the specific binding of hRNase1-EGF to EGFR, the EGFR-deficient H69 cells were incubated with 300 nM of FITC-hRNase1-hEGF or 100 nM of RITC-transferrin.

Table I. *Comparison of relative RNase activity and growth inhibition against A431 cells.*

	Activity (%)	The IC_{50} value against A431 cells (μM)
hRNase1	100	–
hRNase1-hEGF	85	0.55
des.1-7 hRNase1-hEGF	0.34	0.35

Assays for assessing the growth-inhibitory effect of the RNase-EGF fused proteins. The growth-inhibitory effect of the fused proteins was assayed by the colorimetric MTT assay. Exponentially growing A431 and H69 cells were seeded into 96-microwell plates (1500 cells/well) and left to adhere overnight. Serial dilutions of the fused proteins were added and the incubation was continued for a further 80 h. At the end of the incubation period, the cells were washed twice with PBS, treated with a fresh 1:1 mixture of 0.4% MTT in PBS and 0.1 M sodium succinate, and further incubated at 37°C for 3 h. Dimethyl sulfoxide was added to dissolve the MTT crystals, the samples were mixed thoroughly at room temperature and the plates were read with an ELISA reader, at a test wavelength of 570 nm and a reference wavelength of 630 nm. The growth-inhibitory effect of the fused proteins was examined within the concentration range of the fused proteins of 10^{-9} to 10^{-5} M. All the values from quadruplicate assays were averaged and the percentage of surviving cells was calculated *versus* that in the untreated control cell cultures. The average of the background value obtained from the wells without cells was subtracted from all points and defined as 0% cell viability, while the average of all the wells with untreated cells was defined as 100% viability. Comparison of the growth-inhibitory effects of hRNase1-hEGF and des.1-7 hRNase1-hEGF at each concentration was conducted using the *t*-test. *P* values of less than 0.01 were considered to be statistically significant.

Results

Ribonucleolytic activity of the fused proteins against yeast RNA. The relative RNase activity of hRNase1-hEGF was about 85% of that of unfused recombinant hRNase1. On the other hand, the RNase activity of des.1-7 hRNase1-hEGF was 0.34% of that of unfused hRNase1 and 250-fold less than that of hRNase1-hEGF (Table I).

Detection of fluorescence-labelled hRNase1-hEGF in cell culture. Within 30 min, FITC-hRNase1-hEGF was mainly

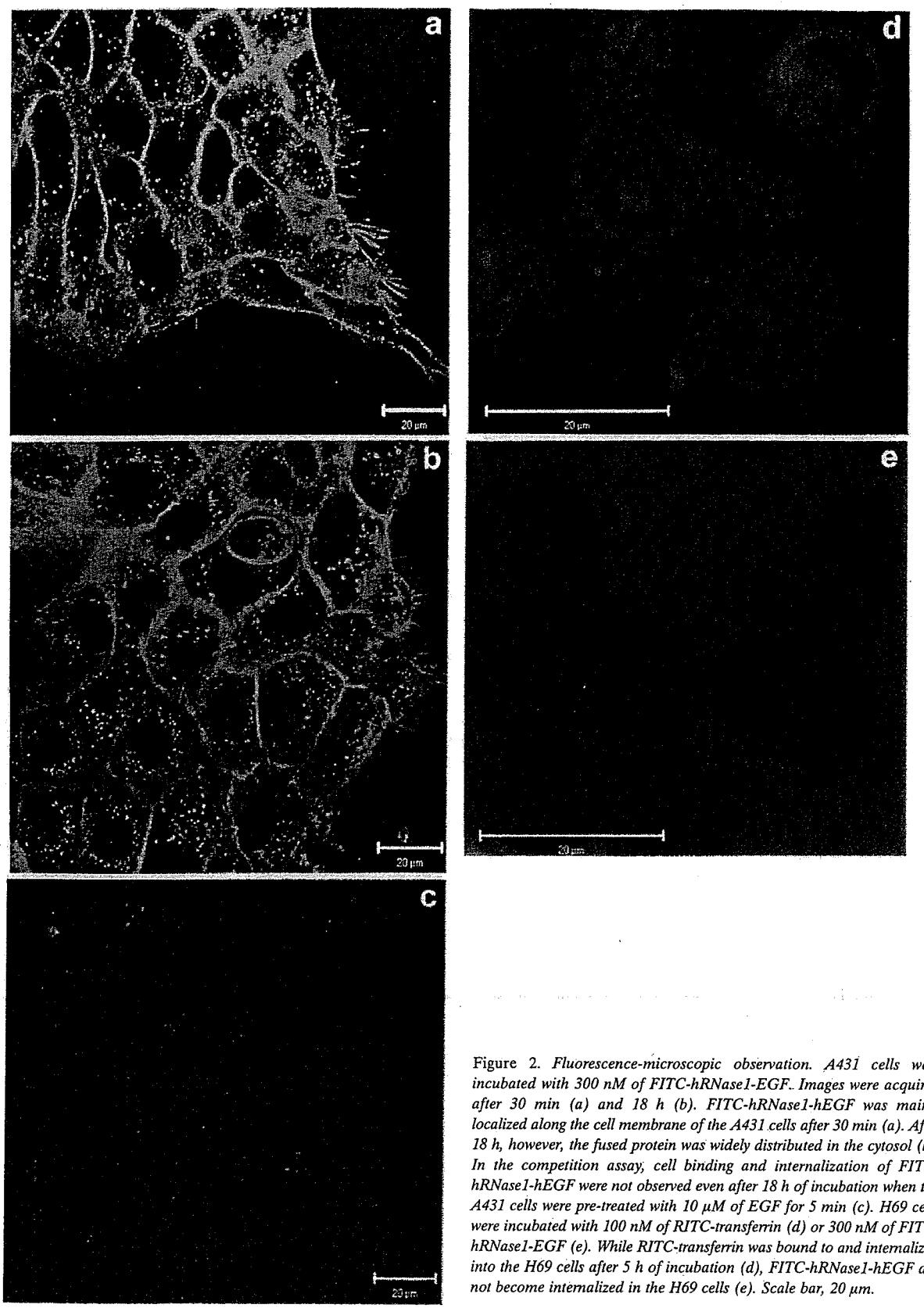

Figure 2. *Fluorescence-microscopic observation. A431 cells were incubated with 300 nM of FITC-hRNase1-EGF. Images were acquired after 30 min (a) and 18 h (b). FITC-hRNase1-hEGF was mainly localized along the cell membrane of the A431 cells after 30 min (a). After 18 h, however, the fused protein was widely distributed in the cytosol (b). In the competition assay, cell binding and internalization of FITC-hRNase1-hEGF were not observed even after 18 h of incubation when the A431 cells were pre-treated with 10 µM of EGF for 5 min (c). H69 cells were incubated with 100 nM of RITC-transferrin (d) or 300 nM of FITC-hRNase1-EGF (e). While RITC-transferrin was bound to and internalized into the H69 cells after 5 h of incubation (d), FITC-hRNase1-hEGF did not become internalized in the H69 cells (e). Scale bar, 20 µm.*

6

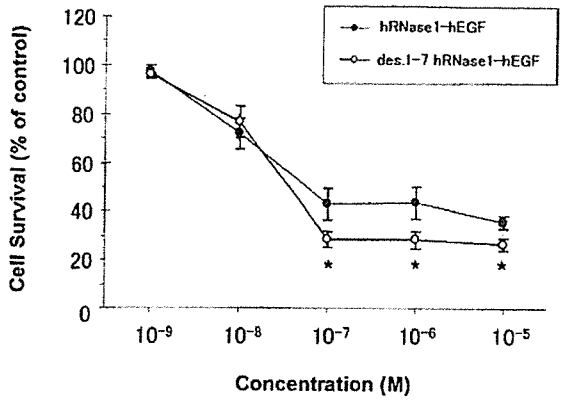

Figure 3. *Growth-inhibitory effect of the fused proteins against the A431 cells. EGFR-overexpressing A431 cells in DMEM supplemented with 10% fetal calf serum were seeded into 96-microwell plates (1500 cells/well) and left to adhere overnight. Various concentrations of hRNase1-hEGF (●) and des.1-7 hRNase1-hEGF (○) were added and the incubation was continued for a further 80 h. The percentage of surviving cells in each well was monitored by MTT assay (% relative to that in the untreated control). All points represent the average of four cultures. *:p<0.01 versus hRNase1-hEGF.*

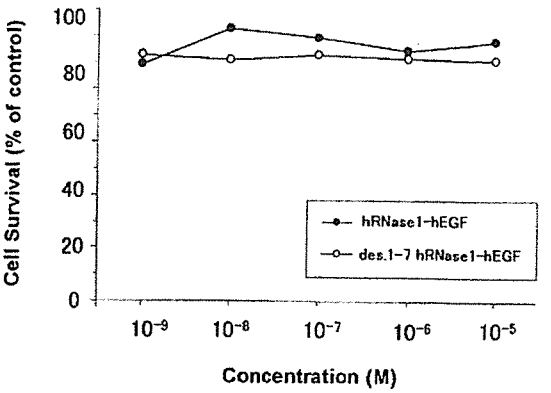

Figure 4. *Growth-inhibitory effect of the fused proteins against the H69 cells. The EGFR-deficient H69 cells were plated (1500 cells/well) and incubated overnight, and were subsequently treated with various concentrations of hRNase1-hEGF (●) and des.1-7 hRNase1-hEGF (○). Cell survival was determined by MTT assay (% relative to that in the untreated control). All points represent the average of quadruplicate determinations.*

localized along the cell membrane of the A431 cells (Figure 2A). By 18 h, FITC-hRNase1-hEGF was widely distributed in the cytosol, but still not associated with the nuclei (Figure 2B). In the competition assay, cell binding and internalization of FITC-hRNase1-hEGF were not observed when the A431 cells were pre-treated with 10 μM of EGF (Figure 2C). While RITC-transferrin was bound to or internalized into H69 cells after 5 h of incubation (Figure 2D), FITC-hRNase1-hEGF was not internalized into H69 cells (Figure 2E).

Growth-inhibitory effect of the fused proteins against the cancer cells. Both of the fused proteins inhibited the growth of the A431 cells which overexpress EGFR, in a dose-dependent manner (Figure 3). The IC_{50} values of hRNase1-hEGF and des.1-7 hRNase1-hEGF were 0.55 and 0.35 μM, respectively, for the A431 cells (Table I). The IC_{50} value of des.1-7 hRNase1-hEGF was approximately 1.5 times lower than that of hRNase1-hEGF. In the concentration range of 10^{-7} to 10^{-5} M, there was a statistically significant difference in the growth-inhibitory effect between hRNase1-hEGF and des.1-7 hRNase1-hEGF (p=0.007, 0.005, 0.002). On the other hand, neither of the fused proteins had any inhibitory effect against H69 cells, which show very weak surface expression of EGFR (Figure 4).

Discussion

We prepared des.1-7 hRNase1-EGF, which is a fused protein of an hRNase1 variant created by partial mutagenesis of the RNase inhibitor binding site and hEGF, in order to evade inhibitor-RNase interaction and allow the RNase to exert more enzymatic activity in the cytosol. The internalization of the fused proteins into EGFR-overexpressing cells was visualized by fluorescence microscopy. Also, a competition assay was conducted to confirm the EGFR-mediated internalization of the fused proteins. *In vitro*, the growth-inhibitory effect of des.1-7 hRNase1-hEGF was statistically significantly more pronounced than that of hRNase1-hEGF against EGFR-overexpressing A431 cells, despite its much weaker RNase activity. The internalization and cell growth-inhibitory activity of the RNase-EGF fused proteins were not observed against EGFR-deficient cells.

Interestingly, highly cationic RNases have been reported to be efficiently adsorbed onto the negatively charged cell surface by electrostatic interaction and internalized into cells (23). These modified cationic RNases were demonstrated to show cytotoxic activity against cells, this cytotoxic activity being correlated with their net positive charge (23). Since the cytotoxic activity of the modified cationic RNases depended on their cell surface adsorption and non-specific internalization, we suggest that RNase-EGF fused proteins may be more suitable for targeted therapy, because of their specific EGFR-mediated internalization.

Complexes of cell surface receptors and their ligands are commonly internalized by endocytosis, to enter the prelysosomal endosomal pathway for further processing. It is well established that EGF-binding to the surface receptor results in down-regulation of EGFR expression. Several authors have described the movement of EGFR into intracellular compartments after EGF-stimulated tyrosine

autophosphorylation. Carpentier *et al.* detected phosphorylated EGFR on A431 cells at the plasma membrane within 1 min of the addition of EGF, and half of all EGFRs were progressively internalized between 10 and 30 min following the addition of an antiphosphotyrosine antibody (24). Hopkins *et al.* demonstrated a progressively increasing number of EGF-EGFR complexes on the internal vesicles of the mulitivesicular bodies in the cells from 3 min after EGF stimulation, and the mulitivesicular bodies packed with these complexes began to accumulate in the pericentriolar area from 20 min following the addition of an antibody to EGFR coupled with FITC or gold labels (25). In the present study, the RNase-EGF fused proteins were mainly localized along the cell membrane of the A431 cells by 30 min, and not in the cytosol. After 18-h incubation, the cell-bound fused proteins were found to be efficiently distributed in the cytosol. These results suggest that the sterical problems of RNase-EGF fused proteins themselves might interfere with the endocytosis and consequently delay the internalization, as compared to that of unfused EGF. Binding of the fused proteins to A431 cells was strongly inhibited in the presence of excess hEGF. Cell-binding and internalization of RNase-EGF fused proteins were not observed in the EGFR-deficient H69 cells, although transferrin, which has been used as a ligand in immunotoxin construction in a number of studies, was internalized into these same cells. These results indicate that the fused proteins bind specifically to cellular EGFR.

Cytosolic RNase inhibitor, which is a 50-kDa protein present in all mammals, binds to and inactivates most members of the RNase A superfamily (26). Several observations suggest that cytosolic RNase inhibitor acts as a sentry to protect mammalian cells from RNases entering the cells from the extracellular fluid. Overproduction of RNase inhibitor has been shown to increase cellular resistance to toxic RNases (27). Recently, it has been reported that HeLa cells with silencing of the cytosolic RNase inhibitor mRNA by RNA interference are more sensitive to cytotoxic RNases as compared to wild-type HeLa cells (28). These findings suggest that, for better clinical application of RNase-based immunotoxins, the RNases should be effectively internalized and exhibit low affinity for the cytosolic RNase inhibitor. We previously demonstrated that hRNase1-hEGF fused protein exerted its cytotoxic effect in a dose-dependent manner against EGFR-overexpressing cells, and that the cytotoxic effect of this fused protein was more potent than that of free hRNase1 and/or free hEGF (19). Des.1-7 hRNase1 is a hRNase1 variant constructed by deleting 7 amino acid residues from the amino-terminus of hRNase1, which is more resistant to the RNase inhibitor, but less active enzymatically (20). In the present study, a genetically fused protein, des.1-7 hRNase1-hEGF was produced, to clarify the mechanisms of the growth-inhibitory activity of the RNase-EGF fused proteins. Surprisingly, des.1-7 hRNase1-hEGF fused protein showed a significantly more potent growth-inhibitory effect than hRNase1-hEGF against EGFR-overexpressing cells, even though the latter had a 250 fold more potent ribonucleolytic activity. This result is consistent with the suggestion that the low affinity of the fused proteins for the cytosolic RNase inhibitor is an important factor in the growth-inhibitory effect of the fused proteins.

In recent years, increasingly more EGFR-targeted cancer therapies are being developed. Gefitinib is an orally active, selective EGFR tyrosine kinase inhibitor, which blocks signal transduction pathways implicated in cell proliferation and survival, and tumor regression or partial radiographic responses were observed in 9 – 12% of patients with heavily pretreated non-small cell lung cancer in clinical trials (29). Cetuximab is a chimeric monoclonal antibody highly selective for EGFR and, in clinical trials, treatment with cetuximab combined with irinotecan, fluorouracil and folinic acid produced partial responses in 43-58% of patients with treatment-naive metastatic colorectal cancer expressing EGFR (30). *In vitro*, the IC_{50} value of gefitinib against A431 cells has been shown to be 0.1 μM, while cetuximab was less potent at suppressing the proliferation of A431 cells than gefitinib (31). We suggest that the growth-inhibitory effect of the RNase-EGF fused proteins is attributable to their residual riboneucleolytic activity in the cytosol in the presence of the cytosolic RNase inhibitor, since the growth-inhibitory effect has been shown to become more potent with modification of the RNase inhibitor binding site. Our current data showed that the IC_{50} value of des. 1-7 hRNase1-hEGF against A431 cells was very close to that of the above-mentioned agents, although the mechanism underlying the growth-inhibitory effect of the RNase-EGF fused proteins is unique and entirely different from that of the new drugs, namely, gefitinib and cetuximab.

In conclusion, RNase-EGF fused proteins show a growth-inhibitory effect against EGFR-overexpressing cells, which is considered to be mediated by receptor-mediated internalization and ribonucleolytic activity of the fused proteins themselves in the cytosol. In addition, the data showed that the growth-inhibitory effect of the RNase-EGF fused proteins may be further improved by modifying the RNase inhibitor-binding site of these proteins.

Acknowledgements

We thank Ms. Yuki Nakamura for her excellent technical assistance. This work was supported, in part, by a Grant-in-Aid from the Ministry of Education, Culture, and Science, Japan.

References

1 Ozawa S, Ueda M, Ando N, Shimizu N and Abe O: Prognostic significance of epidermal growth factor receptor in esophageal squamous cell carcinomas. Cancer *63*: 2169-2173, 1989.